J. Fluid Mech. (1987), *vol.* 174, *pp.* 299–312
Printed in Great Britain

Energy computations for evolution of class I and II instabilities of Stokes waves

By MICHAEL STIASSNIE
Department of Civil Engineering, Technion, Haifa 32000, Israel

AND LEV SHEMER
Faculty of Engineering, Tel-Aviv University, Tel-Aviv 69978, Israel

(Received 5 June 1985 and in revised form 6 January 1986)

The modified Zakharov equation is used to study the coupled evolution of class I and class II instabilities of surface gravity waves on infinitely deep water. In contrast to single class (I or II) evolution, the coupled behaviour is non-periodic. Except for the very steep waves a dominance of class I modes over those of class II is observed. Energy calculations show that the Hamiltonian of the wave field considered is nearly constant. Thus the Zakharov and the modified Zakharov equations represent consistent approximations of the original water-wave problem.

1. Introduction

In Stiassnie & Shemer (1984) we derived a modified version of the Zakharov integral equation for surface gravity waves. This version includes higher-order, class II, nonlinear interaction as well as the more familiar class I interaction. A linear stability analysis of the new equation was used to study some short-time aspects of class I and class II instabilities of a Stokes wave, yielding results in agreement with those of McLean (1982).

1.1. *Class I instability*

Wave flume experiments by Lake *et al.* (1977) have shown how the disturbances grew in time, reached a maximum and then subsided. Furthermore, the experiments showed how the unsteady wavetrain became, at some stage of its evolution, nearly uniform again. Yuen & Lake (1982) used a numerical solution of the Zakharov equation to show that the evolution may be recurring (Fermi–Pasta–Ulam recurrence) or chaotic, depending on the choice of modes included in the calculation. Stiassnie & Kroszynski (1982) used the nonlinear Schrödinger equation to study analytically the evolution of a three-wave system, composed of a carrier and two initially small 'side-band' disturbances. Their recurrence period (given by a simple formula) is in good agreement with the numerical results. For infinitely deep water the most unstable class I disturbances are in the direction of the carrier, so that the instability is essentially two-dimensional.

1.2. *Class II instability*

Experiments by Su (1982) and Su *et al.* (1982) have shown that an initial state of a two-dimensional wavetrain of large steepness evolved into a series of three-dimensional crescentic spilling breakers (class II), and was followed by a transition to a two-dimensional modulated wavetrain (class I). One can speculate that the growth of the crescentic waves and their disappearance are one cycle of a recurring phenomenon. In a recent study (Shemer & Stiassnie 1985), we proved analytically that a wavefield composed of a Stokes wave and two most unstable class II disturbances does also undergo a kind of Fermi–Pasta–Ulam recurrence.

1.3. *Coupled instability*

In two papers Su & Green (1984, 1985) suggested the following interpretation for their recent experimental results: under the initial action of class I instability a wavetrain with moderately high steepness ($a_0 k_0 > 0.12$; a_0, k_0 are the amplitude and wavenumber respectively) may undergo a considerable modulation in its envelope; subsequently, a few of the waves in the middle of the maximum modulation will have local wave steepness high enough to trigger class II instability. They added that for high enough initial steepness ($a_0 k_0 > 0.15$) these locally steeper waves lead to three-dimensional wave breaking.

The main goal of the present work is to provide an approximate mathematical model for the coexistence and interactions of the two classes of instabilities, which appear to be relevant for moderately steep waves. A theoretical study of these processes is pursued using the modified Zakharov equation. The essentials of the derivation of the modified Zakharov equation, pertinent to this study are given in §2 (for details see Stiassnie & Shemer 1984). In our earlier studies (Stiassnie & Kroszynski 1982; Shemer & Stiassnie 1985) we analysed wave fields composed of three free waves, which was the smallest number required in order to model the relevant physical process and keep the mathematics manageable. For the present study of coupled evolution of class I and class II instabilities the smallest required number of free waves is five. The appropriate model for such a system is given in §3. One possible way to check the mathematical model is to calculate the total energy of the wave field, which should be constant in any non-dissipative medium.

The details of the energy calculation are provided in §4. The results are presented in §5. The conclusions, drawn in §6, demonstrate the potential of the modified Zakharov equation as a tool for studying complex water-wave fields.

2. Background

The equations governing the irrotational flow of an incompressible inviscid fluid with a free surface and infinitely deep bottom are:

$$\nabla^2\phi = 0 \quad (z \leqslant \eta(\boldsymbol{x}, t)), \tag{2.1a}$$

$$\left.\begin{aligned} \eta_t + (\nabla\phi\cdot\nabla\eta) - \phi_z &= 0 \\ \phi_t + \tfrac{1}{2}(\nabla\phi)^2 + gz &= 0 \end{aligned}\right\} \quad (z = \eta(\boldsymbol{x}, t)), \tag{2.1b, c}$$

$$|\nabla\phi| \to 0 \quad (z \to -\infty), \tag{2.1d}$$

where $\phi(\boldsymbol{x}, z, t)$ is the velocity potential, $\eta(\boldsymbol{x}, t)$ is the free-surface elevation and g the gravitational acceleration. The horizontal coordinates are $(x_1, x_2) = \boldsymbol{x}$, the vertical coordinate z is pointing upwards, and t is the time.

Given an initial condition in terms of $\eta(\boldsymbol{x}, 0)$, $\phi(\boldsymbol{x}, \eta(\boldsymbol{x}, 0), 0)$, one can transform the problem into an evolution equation in the Fourier plane

$$\mathrm{i}\,\frac{\partial B}{\partial t} = \mathrm{I}_3(\boldsymbol{k}, t) + \mathrm{I}_4(\boldsymbol{k}, t) + \ldots. \tag{2.2}$$

The new dependent variable $B(\boldsymbol{k}, t)$ represents the free components of the wave field. I_3, I_4, ..., are integral operators representing quartet, quintet, ..., nonlinear interaction, respectively.

The leading term on the right-hand side of (2.2) was first derived by Zakharov (1968), and the higher-order term I_4 was obtained in Stiassnie & Shemer (1984):

$$\mathrm{I}_3 = \iiint_{-\infty}^{\infty} T^{(2)}_{0,1,2,3} B_1^* B_2 B_3 \delta_{0+1-2-3} \, \mathrm{e}^{\mathrm{i}(\omega+\omega_1-\omega_2-\omega_3)t} \, \mathrm{d}\boldsymbol{k}_1 \, \mathrm{d}\boldsymbol{k}_2 \, \mathrm{d}\boldsymbol{k}_3, \tag{2.3a}$$

$$\begin{aligned}\mathrm{I}_4 = \iiiint_{-\infty}^{\infty} \{ & U^{(2)}_{0,1,2,3,4} B_1^* B_2 B_3 B_4 \delta_{0+1-2-3-4} \, \mathrm{e}^{\mathrm{i}(\omega+\omega_1-\omega_2-\omega_3-\omega_4)t} \\ & + U^{(3)}_{0,1,2,3,4} B_1^* B_2^* B_3 B_4 \delta_{0+1+2-3-4} \, \mathrm{e}^{\mathrm{i}(\omega+\omega_1+\omega_2-\omega_3-\omega_4)t} \} \, \mathrm{d}\boldsymbol{k}_1 \, \mathrm{d}\boldsymbol{k}_2 \, \mathrm{d}\boldsymbol{k}_3 \, \mathrm{d}\boldsymbol{k}_4,\end{aligned} \tag{2.3b}$$

where we use a compact notation in which the arguments $\boldsymbol{k}_i$ are replaced by the subscript i, with the subscript zero assigned to $\boldsymbol{k}$. ω is related to $\boldsymbol{k}$ through the linear dispersion relation $\omega(\boldsymbol{k}) = (g|\boldsymbol{k}|)^{\frac{1}{2}}$. The kernels $T^{(2)}(\boldsymbol{k}, \boldsymbol{k}_1, \boldsymbol{k}_2, \boldsymbol{k}_3)$, $U^{(2)}(\boldsymbol{k}, \boldsymbol{k}_1, \boldsymbol{k}_2, \boldsymbol{k}_3, \boldsymbol{k}_4)$, ..., as well as other kernels to appear subsequently, are given in Stiassnie & Shemer (1984). The asterisk denotes the complex conjugate. $B(\boldsymbol{k}, t)$ is related to the Fourier transform (denoted by a hat) of $\eta(\boldsymbol{x}, t)$ and $\phi^{\mathrm{s}}(\boldsymbol{x}, t) = \phi(\boldsymbol{x}, \eta(\boldsymbol{x}, t), t)$, the velocity potential at the free surface, through $b(\boldsymbol{k}, t)$, which is a kind of generalized 'amplitude' spectrum

$$\hat{\eta}(\boldsymbol{k}, t) = \left(\frac{\omega}{2g}\right)^{\frac{1}{2}} [b(\boldsymbol{k}, t) + b^*(-\boldsymbol{k}, t)], \tag{2.4a}$$

$$\hat{\phi}^{\mathrm{s}}(\boldsymbol{k}, t) = -\mathrm{i}\left(\frac{g}{2\omega}\right)^{\frac{1}{2}} [b(\boldsymbol{k}, t) - b^*(-\boldsymbol{k}, t)], \tag{2.4b}$$

$$b(\boldsymbol{k}, t) = [B + B' + B'' + B''' + \dots] \, \mathrm{e}^{-\mathrm{i}\omega(k)t}. \tag{2.4c}$$

The quantities B', B'', ..., represent the bound components of the wave field, which are given in terms of B as follows:

Second order

$$\begin{aligned} B' = -\iint_{-\infty}^{\infty} \Bigg\{ & V^{(1)}_{0,1,2} B_1 B_2 \delta_{0-1-2} \frac{\mathrm{e}^{\mathrm{i}(\omega-\omega_1-\omega_2)t}}{\omega-\omega_1-\omega_2} \\ & + V^{(2)}_{0,1,2} B_1^* B_2 \delta_{0+1-2} \frac{\mathrm{e}^{\mathrm{i}(\omega+\omega_1-\omega_2)t}}{\omega+\omega_1-\omega_2} \\ & + V^{(3)}_{0,1,2} B_1^* B_2^* \delta_{0+1+2} \frac{\mathrm{e}^{\mathrm{i}(\omega+\omega_1+\omega_2)t}}{\omega+\omega_1+\omega_2} \Bigg\} \, \mathrm{d}\boldsymbol{k}_1 \, \mathrm{d}\boldsymbol{k}_2. \end{aligned} \tag{2.5a}$$

Third order

$$\begin{aligned} B'' = -\iiint_{-\infty}^{\infty} \Bigg\{ & \tilde{T}^{(1)}_{0,1,2,3} B_1 B_2 B_3 \delta_{0-1-2-3} \frac{\mathrm{e}^{\mathrm{i}(\omega-\omega_1-\omega_2-\omega_3)t}}{\omega-\omega_1-\omega_2-\omega_3} \\ & + (\tilde{T}^{(2)}_{0,1,2,3} - T^{(2)}_{0,1,2,3}) B_1^* B_2 B_3 \delta_{0+1-2-3} \frac{\mathrm{e}^{\mathrm{i}(\omega+\omega_1-\omega_2-\omega_3)t}}{\omega+\omega_1-\omega_2-\omega_3} \\ & + \tilde{T}^{(3)}_{0,1,2,3} B_1^* B_2^* B_3 \delta_{0+1+2-3} \frac{\mathrm{e}^{\mathrm{i}(\omega+\omega_1+\omega_2-\omega_3)t}}{\omega+\omega_1+\omega_2-\omega_3} \\ & + \tilde{T}^{(4)}_{0,1,2,3} B_1^* B_2^* B_3^* \delta_{0+1+2+3} \frac{\mathrm{e}^{\mathrm{i}(\omega+\omega_1+\omega_2+\omega_3)t}}{\omega+\omega_1+\omega_2+\omega_3} \Bigg\} \, \mathrm{d}\boldsymbol{k}_1 \, \mathrm{d}\boldsymbol{k}_2 \, \mathrm{d}\boldsymbol{k}_3. \end{aligned} \tag{2.5b}$$

Fourth order

$$B''' = -\iiiint_{-\infty}^{\infty}\left\{\tilde{U}^{(1)}_{0,1,2,3,4} B_1 B_2 B_3 B_4 \delta_{0-1-2-3-4} \frac{e^{i(\omega-\omega_1-\omega_2-\omega_3-\omega_4)t}}{\omega-\omega_1-\omega_2-\omega_3-\omega_4}\right.$$
$$+(\tilde{U}^{(2)}_{0,1,2,3,4}-U^{(2)}_{0,1,2,3,4}) B_1^* B_2 B_3 B_4 \delta_{0+1-2-3-4} \frac{e^{i(\omega+\omega_1-\omega_2-\omega_3-\omega_4)t}}{\omega+\omega_1-\omega_2-\omega_3-\omega_4}$$
$$+(\tilde{U}^{(3)}_{0,1,2,3,4}-U^{(3)}_{0,1,2,3,4}) B_1^* B_2^* B_3 B_4 \delta_{0+1+2-3-4} \frac{e^{i(\omega+\omega_1+\omega_2-\omega_3-\omega_4)t}}{\omega+\omega_1+\omega_2-\omega_3-\omega_4}$$
$$+\tilde{U}^{(4)}_{0,1,2,3,4} B_1^* B_2^* B_3^* B_4 \delta_{0+1+2+3-4} \frac{e^{i(\omega+\omega_1+\omega_2+\omega_3-\omega_4)t}}{\omega+\omega_1+\omega_2+\omega_3-\omega_4}$$
$$\left.+\tilde{U}^{(5)}_{0,1,2,3,4} B_1^* B_2^* B_3^* B_4^* \delta_{0+1+2+3+4} \frac{e^{i(\omega+\omega_1+\omega_2+\omega_3+\omega_4)t}}{\omega+\omega_1+\omega_2+\omega_3+\omega_4}\right\} dk_1\, dk_2\, dk_3\, dk_4. \quad (2.5c)$$

3. The evolution equations for a system composed of five free waves

In the present study we restrict the discussion to wave fields which consist of five free components:

$$\eta = \sum_{n=1}^{5} a_n \cos\left(\boldsymbol{k}_n \cdot \boldsymbol{x} - \int_0^t \Omega_n\, dt + \theta_n\right) + \text{higher-order bound components.} \quad (3.1)$$

The wave (1) is the leading component of the original Stokes wave, to be called 'the carrier'. The two couples (2, 3) and (4, 5) were chosen to be the most unstable disturbances of class I and class II instabilities respectively.

These most unstable disturbances were obtained by a linear stability analysis (see Stiassnie & Shemer 1984). The wavenumbers of these five waves are

$$\left.\begin{aligned} \boldsymbol{k}_1 = k_0(1,0), \quad \boldsymbol{k}_2 = k_0(1+p_{\mathrm{I}},0), \quad \boldsymbol{k}_4 = k_0(1{,}5,q_{\mathrm{II}}),\\ \boldsymbol{k}_3 = k_0(1-p_{\mathrm{I}},0) \quad \boldsymbol{k}_5 = k_0(1{,}5,-q_{\mathrm{II}}),\end{aligned}\right\} \quad (3.2)$$

The numerical values of p_{I} and q_{II} are provided by the linear stability analysis.

The initial amplitudes and phase shifts of these waves are chosen to be as follows:

$$\left.\begin{aligned} a_1(0) &= a_0,\\ a_2(0) = a_3(0) &= \epsilon_{\mathrm{I}} a_0 \quad (\epsilon_{\mathrm{I}} = o(1)),\\ a_4(0) = a_5(0) &= \epsilon_{\mathrm{II}} a_0 \quad (\epsilon_{\mathrm{II}} = o(1)),\end{aligned}\right\} \quad (3.3)$$

$$\theta_1(0) = 0, \quad \theta_2(0) = \theta_3(0) = \theta_{\mathrm{I}}, \quad \theta_4(0) = \theta_5(0) = \theta_{\mathrm{II}}. \quad (3.4)$$

The 'Stokes-corrected' frequencies Ω_n are given by:

$$\Omega_n = \omega_n + T_{nnnn}|B_n|^2 + 2\sum_{m\neq n} T_{nmnm}|B_m|^2. \quad (3.5)$$

The variables B_n are related to these quantities through

$$B_n(t) = \pi\left(\frac{2g}{\omega_n}\right)^{\frac{1}{2}} a_n \exp i\left(\int_0^t (\omega_n - \Omega_n)\, dt + \theta_n\right), \quad (3.6)$$

and satisfy the following discretized version of (2.2):

$$\mathrm{i}\,\frac{\mathrm{d}B_1}{\mathrm{d}t} = (\Omega_1-\omega_1)\,B_1+2T_{1123}\,B_1^*\,B_2\,B_3\,\mathrm{e}^{\mathrm{i}\Omega_\mathrm{I}\,t}+2U^{(3)}_{11145}(B_1^*)^2\,B_4\,B_5\,\mathrm{e}^{\mathrm{i}\Omega_\mathrm{II}\,t} + 2(U^{(3)}_{12345}+U^{(3)}_{13245})\,B_2^*\,B_3^*\,B_4\,B_5\,\mathrm{e}^{\mathrm{i}(\Omega_\mathrm{II}-\Omega_\mathrm{I})\,t}, \tag{3.7a}$$

$$\mathrm{i}\,\frac{\mathrm{d}B_2}{\mathrm{d}t} = (\Omega_2-\omega_2)\,B_2+T_{2311}\,B_3^*\,B_1^2\,\mathrm{e}^{-\mathrm{i}\Omega_\mathrm{I}\,t}+2(U^{(3)}_{23145}+U^{(3)}_{21345})\,B_1^*\,B_3^*\,B_4\,B_5\,\mathrm{e}^{\mathrm{i}(\Omega_\mathrm{II}-\Omega_\mathrm{I})\,t}, \tag{3.7b}$$

$$\mathrm{i}\,\frac{\mathrm{d}B_3}{\mathrm{d}t} = (\Omega_3-\omega_3)\,B_3+T_{3211}\,B_2^*\,B_1^2\,\mathrm{e}^{-\mathrm{i}\Omega_\mathrm{I}\,t}+2(U^{(3)}_{31245}+U^{(3)}_{32145})\,B_1^*\,B_2^*\,B_4\,B_5\,\mathrm{e}^{\mathrm{i}(\Omega_\mathrm{II}-\Omega_\mathrm{I})\,t}, \tag{3.7c}$$

$$\begin{aligned}\mathrm{i}\,\frac{\mathrm{d}B_4}{\mathrm{d}t} &= (\Omega_4-\omega_4)\,B_4+U^{(2)}_{45111}\,B_5^*\,B_1^3\,\mathrm{e}^{-\mathrm{i}\Omega_\mathrm{II}\,t}\\ &\quad+(U^{(2)}_{45123}+U^{(2)}_{45132}+U^{(2)}_{45213}+U^{(2)}_{45231}+U^{(2)}_{45312}+U^{(2)}_{45321})\,B_5^*\,B_1\,B_2\,B_3\,\mathrm{e}^{\mathrm{i}(\Omega_\mathrm{I}-\Omega_\mathrm{II})\,t},\end{aligned} \tag{3.7d}$$

$$\begin{aligned}\mathrm{i}\,\frac{\mathrm{d}B_5}{\mathrm{d}t} &= (\Omega_5-\omega_5)\,B_5+U^{(2)}_{54111}\,B_4^*\,B_1^3\,\mathrm{e}^{-\mathrm{i}\Omega_\mathrm{II}\,t}\\ &\quad+(U^{(2)}_{54123}+U^{(2)}_{54132}+U^{(2)}_{54213}+U^{(2)}_{54231}+U^{(2)}_{54312}+U^{(2)}_{54321})\,B_4^*\,B_1\,B_2\,B_3\,\mathrm{e}^{\mathrm{i}(\Omega_\mathrm{I}-\Omega_\mathrm{II})\,t},\end{aligned} \tag{3.7e}$$

where

$$\Omega_\mathrm{I} = 2\omega_1-\omega_2-\omega_3, \quad \Omega_\mathrm{II} = 3\omega_1-\omega_4-\omega_5. \tag{3.8}$$

From (3.6), (3.3) and (3.4):

$$B_1(0) = \pi\left(\frac{2g}{\omega_1}\right)^{\frac{1}{2}} a_0, \tag{3.9a}$$

$$B_2(0) = \pi\left(\frac{2g}{\omega_2}\right)^{\frac{1}{2}} \epsilon_\mathrm{I}\,a_0\,\exp\mathrm{i}(\theta_\mathrm{I}), \tag{3.9b}$$

$$B_3(0) = \pi\left(\frac{2g}{\omega_3}\right)^{\frac{1}{2}} \epsilon_\mathrm{I}\,a_0\,\exp\mathrm{i}(\theta_\mathrm{I}), \tag{3.9c}$$

$$B_4(0) = \pi\left(\frac{2g}{\omega_4}\right)^{\frac{1}{2}} \epsilon_\mathrm{II}\,a_0\,\exp\mathrm{i}(\theta_\mathrm{II}), \tag{3.9d}$$

$$B_5(0) = \pi\left(\frac{2g}{\omega_5}\right)^{\frac{1}{2}} \epsilon_\mathrm{II}\,a_0\,\exp\mathrm{i}(\theta_\mathrm{II}). \tag{3.9e}$$

The system of 5 nonlinear complex ordinary differential equations (3.7) together with the initial values (3.9) form the evolution problem to be studied.

In Shemer & Stiassnie (1985) we looked at two degenerated forms of the system (3.7). The first dealt with class I instabilities only ($B_4 \equiv B_5 \equiv 0$), and the second was restricted to class II instabilities ($B_2 \equiv B_3 \equiv 0$). For each of these cases the system (3.7) is reduced to a system of 3 complex equations. In Shemer & Stiassnie (1985) we transformed these reduced systems into one real equation in a new variable and solved the resulting equation analytically, in terms of Jacobian elliptic and related functions. We have not succeeded in finding a similar trick for the more general case considered here, and therefore solve the system (3.7) numerically, using the Gil form of the Runge–Kutta method (James, Smith & Wolford 1977).

The numerical scheme is checked by comparing the results obtained for different integration steps. All our numerical results are accurate to five significant digits.

Another approach for checking the mathematical model and the numerical results is to calculate the total energy of the wave field, as elaborated in the following section. Note that this 'energy approach' would still hold when more than 5 free components are included.

4. Energy balance

The exact equations of motion for water-waves (2.1) form a Hamiltonian system as shown by Zakharov (1968), Miles (1977) and Milder (1977), and the total energy of the entire wave field is conserved. The average energy density, taken over the (x_1, x_2)-plane, is given by:

$$h = \lim_{L\to\infty} \frac{1}{(2L)^2} \int_{-L}^{L} \int_{-L}^{L} \frac{1}{2}\left(g\eta^2 + \phi^s \frac{\partial \eta}{\partial t}\right) dx_1\, dx_2. \tag{4.1}$$

Any exact solution should give h = constant, for all t (as long as the waves do not break). When a truncated version of (2.2) is used, one can expect (4.1) to yield $h(t)$, which is only approximately constant. From (2.4a), (2.4b) and (2.5) and the assumption of five free waves:

$$\eta = \frac{1}{2\pi} \sum_{n=1}^{3705} \left(\frac{\omega_n}{2g}\right)^{\frac{1}{2}} [\tilde{B}_n\, e^{i(\boldsymbol{k}_n \cdot \boldsymbol{x} + \chi_n t)} + \text{c.c.}], \tag{4.2}$$

$$\phi^s = \frac{-i}{2\pi} \sum_{n=1}^{3705} \left(\frac{g}{2\omega_n}\right)^{\frac{1}{2}} [\tilde{B}_n\, e^{i(\boldsymbol{k}_n \cdot \boldsymbol{x} + \chi_n t)} - \text{c.c.}], \tag{4.3}$$

where $\tilde{B}_n = B_n$, and $\chi_n = -\omega_n$ for $n = 1, 2, \ldots, 5$ (the five free waves). For $n = 6, 7, \ldots, 3705$, $\tilde{B}_n$ and χ_n are given in the Appendix. The total number of waves considered (3705) results from the structure of (2.5a, b, c); ($3705 = 5 + 3\cdot 5^2 + 4\cdot 5^3 + 5\cdot 5^4$).

Substituting (4.2) and (4.3) into (4.1) gives:

$$\begin{aligned} h = &\sum_{m=1}^{3705} \sum_{n=1;\, \boldsymbol{k}_n = \boldsymbol{k}_m}^{3705} (\omega_m - \chi_n)\, \text{Re}\{\tilde{B}_m \tilde{B}_n^*\, e^{i(\chi_m - \chi_n) t}\} \\ &+ \sum_{m=1}^{3705} \sum_{n=1;\, \boldsymbol{k}_n = -\boldsymbol{k}_m}^{3705} (\omega_m + \chi_n)\, \text{Re}\{\tilde{B}_m \tilde{B}_n\, e^{i(\chi_m + \chi_n) t}\} + \Delta_4 + \Delta_5, \end{aligned} \tag{4.4a}$$

where Δ_4 and Δ_5 are terms of order $(a_0 k_0)^4$ and $(a_0 k_0)^5$ respectively, given by:

$$\begin{aligned} \Delta_4 = &\sum_{n=1}^{5} \sum_{m=1,\, m\neq n}^{5} T_{mnmn} |B_m|^2 |B_n|^2 + \sum_{n=1}^{5} T_{nnnn} |B_n|^4 \\ &+ (2T_{1123} + T_{2311} + T_{3211})\, \text{Re}\{(B_1^*)^2 B_2 B_3\, e^{i\Omega_I t}\}, \end{aligned} \tag{4.4b}$$

$$\begin{aligned} \Delta_5 = &(2U^{(3)}_{11145} + U^{(2)}_{45111} + U^{(2)}_{54111})\, \text{Re}\{(B_1^*)^3 B_4 B_5\, e^{i\Omega_{II} t}\} \\ &+ 2(U^{(3)}_{12345} + U^{(3)}_{13245} + U^{(3)}_{23145} + U^{(3)}_{21345})\, \text{Re}\{B_1^* B_2^* B_3^* B_4 B_5\, e^{i(\Omega_{II} - \Omega_I) t}\} \\ &+ (U^{(2)}_{45123} + U^{(2)}_{45132} + U^{(2)}_{45213} + U^{(2)}_{45231} + U^{(2)}_{45312} + U^{(2)}_{45321} + U^{(2)}_{54123} + U^{(2)}_{54132} \\ &+ U^{(2)}_{54213} + U^{(2)}_{54231} + U^{(2)}_{54312} + U^{(2)}_{54321})\, \text{Re}\{B_4^* B_5^* B_1 B_2 B_3\, e^{i(\Omega_I - \Omega_{II}) t}\}. \end{aligned} \tag{4.4c}$$

Note that the conditions that $\boldsymbol{k}_n = \boldsymbol{k}_m$ or $\boldsymbol{k}_n = -\boldsymbol{k}_m$ drastically reduce the number of pairs which contribute to the average energy density. The actual number of contributing wave pairs turns out to be somewhat smaller than 1000 out of a total of 3705^2 possible combinations.

In addition to the contributions of Δ_4 and Δ_5 the accuracy of (4.4*a*) is related to the accuracy of the 'amplitudes' $\tilde{B}_n$. To obtain h accurate to order $(a_0 k_0)^2$, $\tilde{B}_n$ should be accurate to order $(a_0 k_0)$, thus all the $\tilde{B}_n$ in (4.4*a*) except for the first five are set to zero. One can show that the restrictions $\boldsymbol{k}_n = \pm \boldsymbol{k}_m$ exclude the possibility of products having the order $(k_0 a_0)^3$. This means that the result from (4.4*a*) obtained by using only the five free waves is accurate to order $(k_0 a_0)^3$ and has an error of order $(k_0 a_0)^4$. We denote this result by h_3.

$$h_3 = \frac{1}{4\pi^2} \sum_{n=1}^{5} \omega_n |B_n|^2 = \tfrac{1}{2} g \sum_{n=1}^{5} a_n^2. \tag{4.5}$$

For higher-order corrections one has to include the bound waves. To obtain h_4 (h accurate to order $(a_0 k_0)^4$) the first 580 $\tilde{B}_n$ are required; these include B, B', B'' and yield products of B with B'' and B' with B'. h_5 is obtained when all the 3705 $\tilde{B}_n$ are included; thus adding products of B with B''' and B' with B''. Note that in order to obtain an accuracy higher than h_5 one has to add higher-order terms on the right-hand side of (2.2).

5. Results

5.1. *Coupled evolution*

In figure 1 we show the variation with time of the amplitudes of the free waves for class I instability (in the upper row), class II instability (in the middle row) and the coupled instability (in the lower row). The results are for three different Stokes waves having initial steepness $k_0 a_0 = 0.130$ (in the left column), $k_0 a_0 = 0.227$ (middle column), and $k_0 a_0 = 0.366$ (right column). For each of these three Stokes waves we introduce initial disturbances at the most unstable class I and class II modes (see 3.2) defined by the following parameters:

$k_0 a_0$	p_{I}	q_{II}
0.130	0.22	1.62
0.227	0.34	1.51
0.336	0.47	1.30

The curve (1) is for the carrier amplitude, the curves (2), (3) are those for the amplitudes of the most unstable class I disturbances and the curves (4), (5) which coalesce for the present problem, are for the most unstable class II disturbances. All nine figures have a duration of about 400 carrier periods. Both single-class evolutions are periodic and show a substantial decrease in the recurrence period with the increase of the initial carrier steepness. More details about single-class evolution can be found in Shemer & Stiassnie (1985).

The results for the coupled evolutions are non-periodic; this can also be seen from figure 2, which gives the power spectra of $a_1(t)$ for $k_0 a_0 = 0.130$. We have chosen to demonstrate the results for $k_0 a_0 = 0.130$ rather than those for higher steepness (which are qualitatively similar), since this enables us to avoid the complications involved in the question of wave breaking. According to experimental results of Su & Green (1984) no breaking is expected as long as $a_0 k_0 < 0.15$.

The spectra were calculated from records having a duration sixty times longer than that in figure 1. These records are divided into four equal parts, each having 1024 data points. The curves in figure 2 are the average of four power spectra each calculated from one of these parts. The periodicity of the single-class evolutions manifests itself in the distinct equally spaced peaks in figure 2 (*a* and *b*). In figure 2 (*c*)

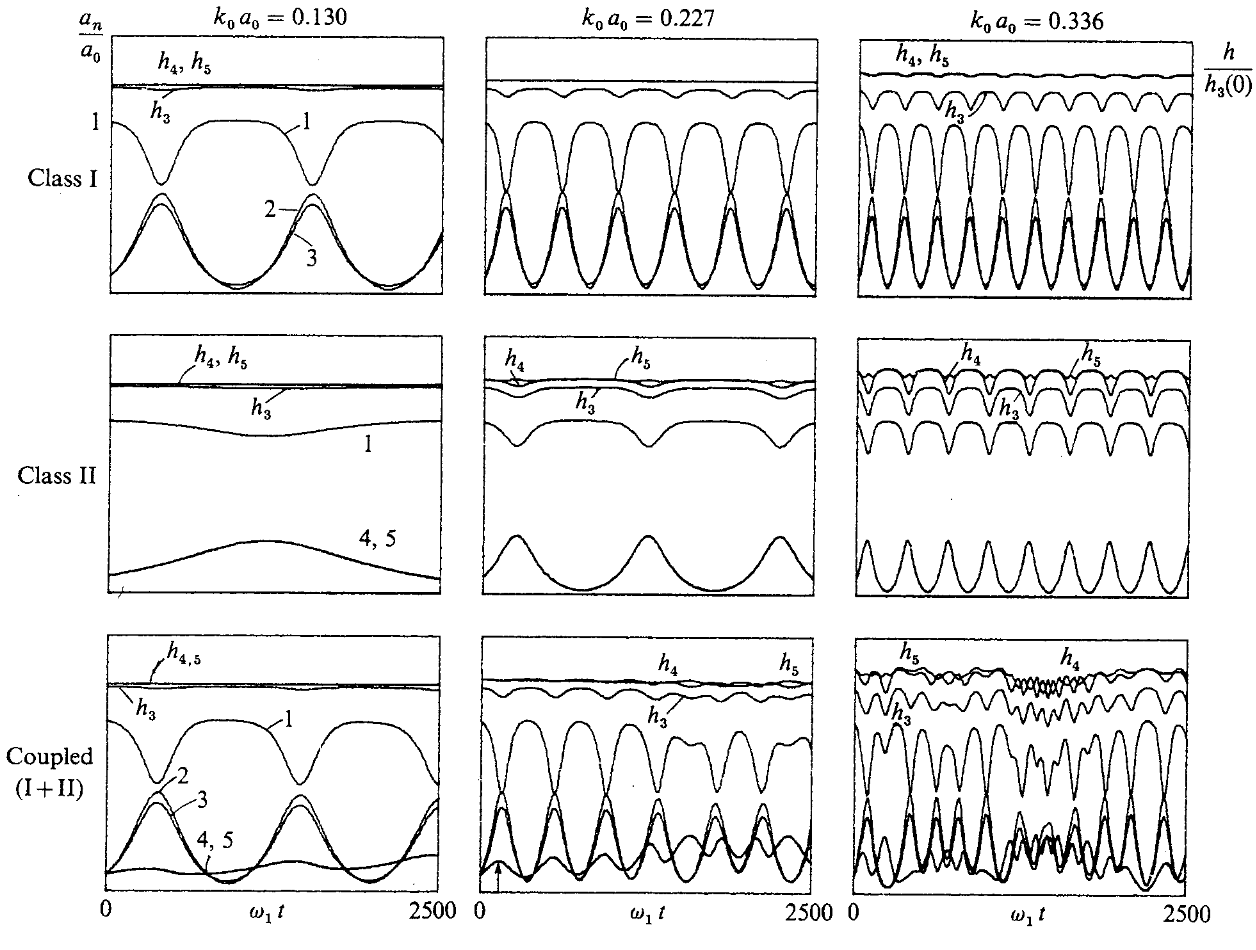

FIGURE 1. Dependence of the evolution process on the carrier steepness ($k_0 a_0$) for $\epsilon_{\mathrm{I}} = \epsilon_{\mathrm{II}} = 0.1$ and $\theta_{\mathrm{I}} = \theta_{\mathrm{II}} = -\frac{1}{4}\pi$.

one can identify only the trace of the first class I peak (figure 2a); there is no identifiable trace of the class II peaks. The spectra for steeper waves are qualitatively similar. The above observation as well as the fact that the amplitudes a_2, a_3 are in general larger than a_4, a_5 (see lowest row of figure 1) can lead to the conclusion that class I instabilities dominate the coupled process. From the point of view of the observer of the water surface this conclusion may be somewhat misleading, since the three-dimensional class II modes seem to catch the observer's eye more than the two-dimensional class I modulations. This is demonstrated in figure 3, which is a picture of the free surface taken at the instant marked with an arrow in the lower row of figure 1.

In figure 4 we present the coupled evolution for $k_0 a_0 = 0.130$, $\theta_{\mathrm{I}} = \theta_{\mathrm{II}} = -\frac{1}{4}\pi$, and for four different couples of initial relative amplitudes of the class I and class II disturbance modes (ϵ_{I}, ϵ_{II}, see (3.3)). A general dominance of class I over class II is observed. In one of the cases ($\epsilon_{\mathrm{I}} = 0.1$, $\epsilon_{\mathrm{II}} = 0.01$) class II is suppressed by class I throughout the evolution, which covers about 1200 wave periods. A similar phenomenon appears for cases with higher values of $k_0 a_0$. Whenever class II disturbances take an active part, their maximum amplitude attained in the course of evolution is essentially independent of the size of the initial disturbance. On the other hand, the time required to attain this maximum depends significantly on ϵ_{I} and ϵ_{II}. The class I dominance also manifests itself by the fact that the amplitudes of class II modes (4, 5) oscillate with the characteristic frequency of class I modes (2, 3).

In order to have a closer look at the parameters which influence the growth or

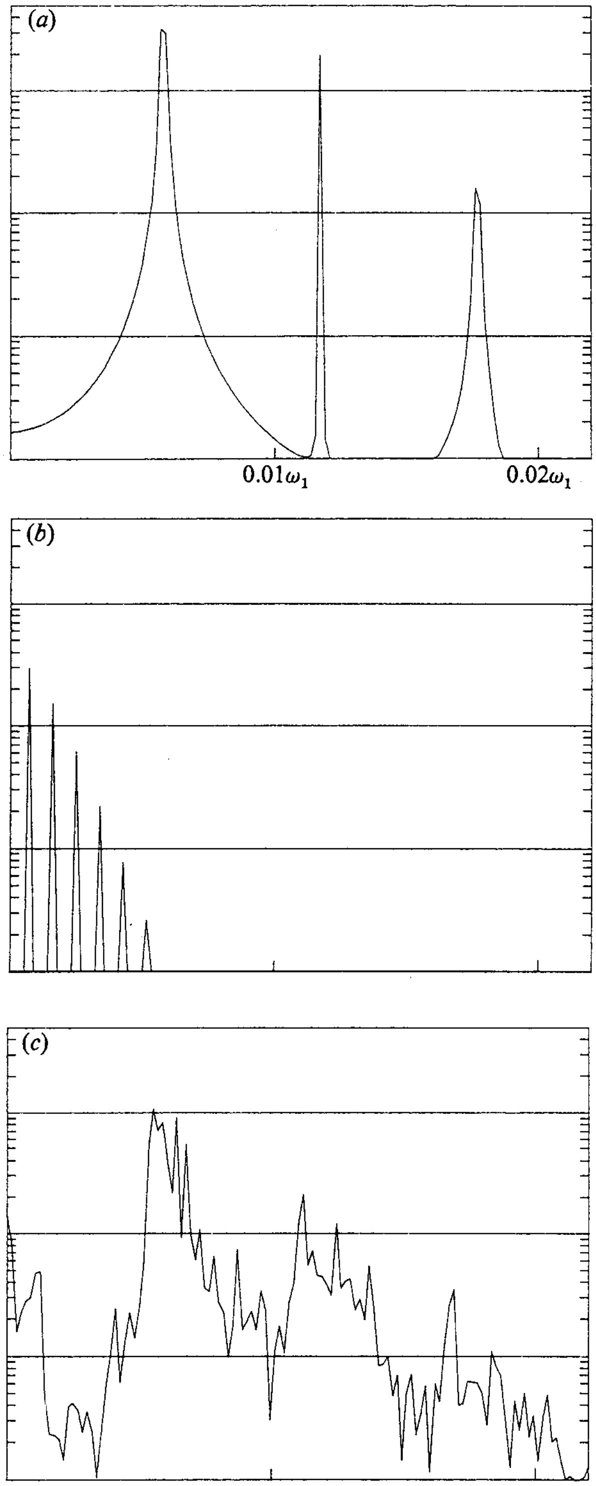

FIGURE 2. Power spectra of the amplitude of the carrier $a_1(t)$ for $k_0 a_0 = 0.130$. (*a*) class I, $\epsilon_{\mathrm{I}} = 0.1$, $\theta_{\mathrm{I}} = -\frac{1}{4}\pi$; (*b*) class II, $\epsilon_{\mathrm{II}} = 0.1$, $\theta_{\mathrm{II}} = -\frac{1}{4}\pi$; (*c*) coupled, $\epsilon_{\mathrm{I}} = \epsilon_{\mathrm{II}} = 0.1$; $\theta_{\mathrm{I}} = \theta_{\mathrm{II}} = -\frac{1}{4}\pi$.

suppression of class II disturbances we study the coupled evolution process for a fixed value of $\epsilon_{\mathrm{I}} = 0.1$ and varying values of ϵ_{II}, and of the initial phase shifts θ_{I} and θ_{II}. We demonstrate some representative results in figure 5 (for $k_0 a_0 = 0.130$) and in figure 6 (for $k_0 a_0 = 0.227$). Both figures have two columns, the left one for $\theta_{\mathrm{I}} = \frac{1}{4}\pi$ and $\theta_{\mathrm{II}} = -\frac{1}{4}\pi$; and the right column for $\theta_{\mathrm{I}} = -\frac{1}{4}\pi$ and $\theta_{\mathrm{II}} = \frac{1}{4}\pi$. These phase values are chosen since they correspond to the two possible extreme values of the initial growth rates (see Shemer & Stiassnie 1985). For $k_0 a_0 = 0.130$ (see figure 5), the

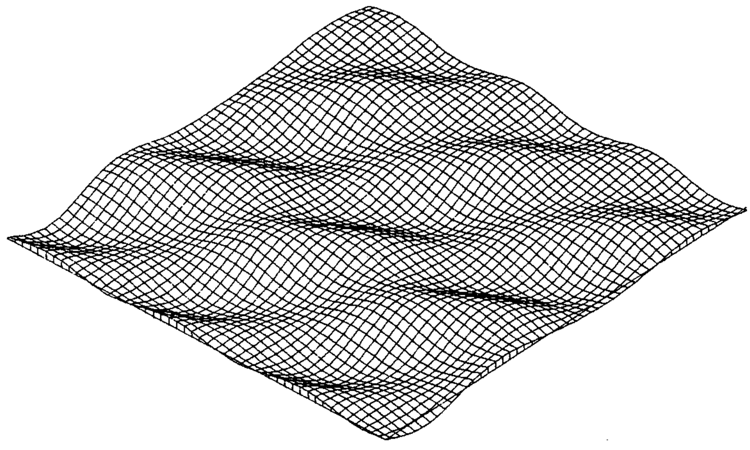

FIGURE 3. Free-surface elevation for $k_0 a_0 = 0.227$, $\epsilon_{\mathrm{I}} = \epsilon_{\mathrm{II}} = 0.1$, $\theta_{\mathrm{II}} = \theta_{\mathrm{II}} = -\frac{1}{4}\pi$, at $\omega_1 t = 150$.

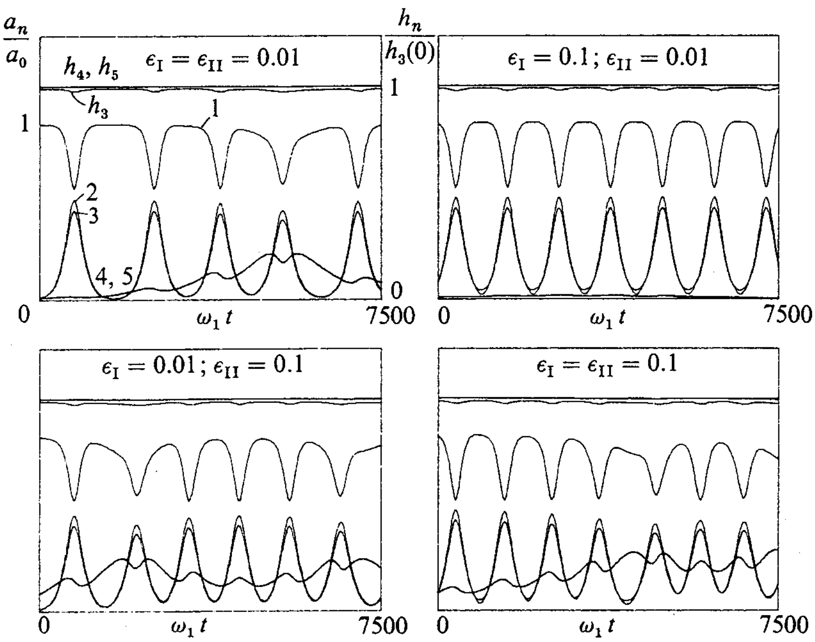

FIGURE 4. Dependence of the evolution process on the amplitudes of the initial disturbances ϵ_{I} and ϵ_{II} for $k_0 a_0 = 0.130$, $\theta_{\mathrm{I}} = \theta_{\mathrm{II}} = -\frac{1}{4}\pi$.

evolution pattern does not seem to be sensitive to the initial phases, and depends primarily on ϵ_{II}. For $\epsilon_{\mathrm{II}} = 0.02$ and lower values, class II instabilities do not grow. For $\epsilon_{\mathrm{II}} > 0.025$ the class II disturbances eventually attain their maximum value. The details for this growth depend on the initial phases; whenever class II disturbances start growing at $t = 0$ they attain their maximum faster.

For $k_0 a_0 = 0.227$, as in the previous case, no significant class II activity appears as long as $\epsilon_{\mathrm{II}} < 0.02$. For $\epsilon_{\mathrm{II}} > 0.02$ a profound difference between the two phases can be observed in figure 6, for $\theta_{\mathrm{I}} = -\theta_{\mathrm{II}} = \frac{1}{4}\pi$ class II modes scarcely participate in the evolution process, whereas for $\theta_{\mathrm{I}} = -\theta_{\mathrm{II}} = -\frac{1}{4}\pi$ these modes are much more active. For $\theta_{\mathrm{I}} = -\theta_{\mathrm{II}} = -\frac{1}{4}\pi$ a small increase in ϵ_{II} changes the pattern significantly (see right column in figure 6). Note that the influence of the initial phase shifts for $k_0 a_0 = 0.227$ is opposite to that observed for $k_0 a_0 = 0.130$; for $k_0 a_0 = 0.227$ class II disturbances develop faster when they initially decrease.

5.2. *Energy conservation*

The uppermost curves in figures 1 and 4–6 represent three approximations of the average energy density, i.e. h_3, h_4 and h_5.

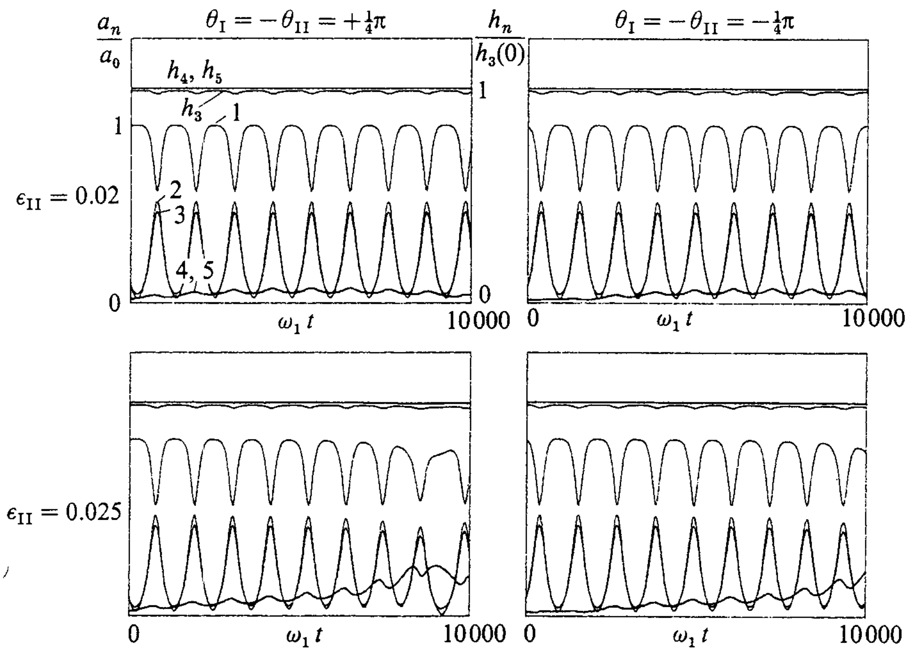

FIGURE 5. Dependence of the evolution process on the amplitude of the initial disturbance ϵ_{II} and the phase angles θ_{I} and θ_{II} for $k_0 a_0 = 0.130$, $\epsilon_{\mathrm{I}} = 0.1$.

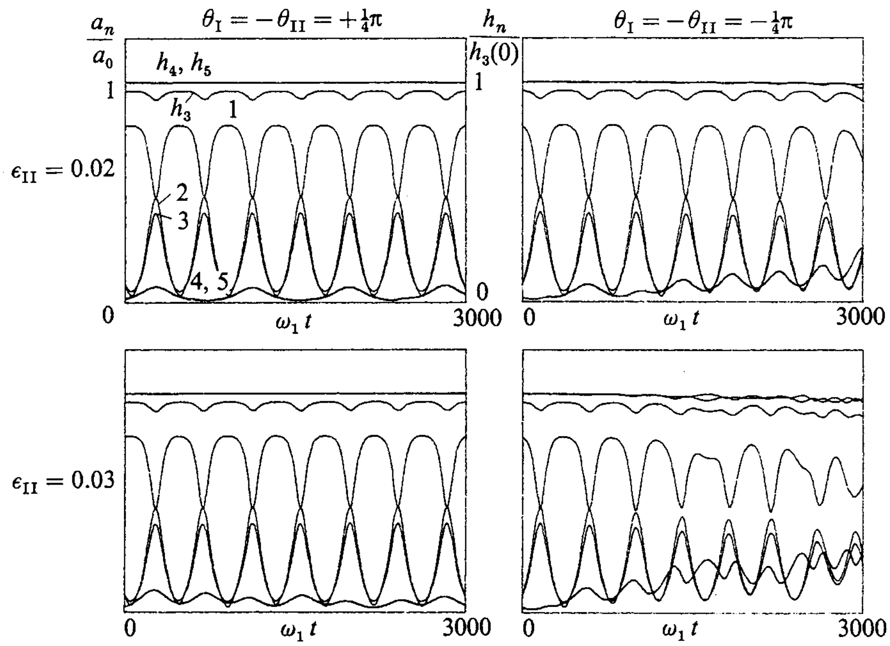

FIGURE 6. Dependence of the evolution process on the amplitude of the initial disturbance ϵ_{II} and the phase angles θ_{I} and θ_{II} for $k_0 a_0 = 0.227$, $\epsilon_{\mathrm{I}} = 0.1$.

Class I interaction: One can see that the contribution of the energy terms of the order $(k_0 a_0)^4$ leads to a considerable improvement in the conservation of the calculated energy in the evolution process, and h_4 does not deviate practically from a horizontal curve, with the exception of the highest amplitude considered. The higher-order h_5 curve does not differ from h_4.

Class II interaction: The middle row of figure 1 shows that the addition of the energy terms of the order $(k_0 a_0)^4$ changes only the 'mean level' of the energy density. In order to obtain improvement in the energy conservation one has to take into account higher-order $(k_0 a_0)^5$ terms. Note that these terms are not necessarily positive and the h_4 and h_5 curves intersect.

Coupled (class I+class II) interaction: For the lowest amplitude considered $(k_0 a_0 = 0.13)$ the curves h_4 and h_5 hardly differ from each other and from the horizontal straight line, giving an improvement compared to h_3. For $k_0 a_0 = 0.227$, h_4 and h_5 give considerably better results than h_3, but some deviations from a horizontal line are seen. The deviations in h_5 are considerably smaller than those in h_4. At even higher amplitude, $k_0 a_0 = 0.336$, h_5 is still better than h_4 but it seems that the present order of approximation is not sufficient.

6. Concluding remarks

The Zakharov equation, first derived by Zakharov in 1968, and the modified Zakharov equation (Stiassnie & Shemer 1984), are two consecutive approximations of the classic water-wave problem, see (2.1). In the derivation of these equations certain assumptions, as well as some rather tedious algebra are involved. The accuracy of these equations for short-time predictions was tested in Stiassnie & Shemer (1984), where the results of a linear stability analysis were found to agree with the exact solution by McLean (1982). In the present paper we extend our analysis to long-time processes. To the best of our knowledge, there is no published theoretical work dealing with processes similar to those considered here. Thus we examine the validity of our solutions by resorting to energy considerations. Since the Zakharov equations are approximate models of a Hamiltonian system, one expects that they conserve energy to their respective order. The present results indeed indicate that the original Zakharov equation conserves energy with a relative error of $O(\epsilon^3)$, while the modified Zakharov equation yields a relative error of $O(\epsilon^4)$, in the averaged energy density. Note that the conclusion of Yuen & Lake (1982 p. 196) that the Zakharov approximation does not conserve energy stems from the fact that they refer to h_3 (see our (4.5)) and do not take into account the higher-order approximation.

Another way to assess the relevance of the obtained solution to real water-waves is to compare our predictions with experimental observations. The available experimental results, Su & Green (1984, 1985), do not provide all the details regarding the initial noise level necessary for quantitative comparison. However, the general pattern of our theoretical results is similar to their experimental observations. In all the cases considered here, class I instabilities are dominant throughout the initial stages of evolution (note that the extent of the experimental facility corresponds to our $\omega_1 t < 1000$). Su & Green (1984) suggest that class I modulations, which start first, trigger the class II instability. While our approach does not support the trigger mechanism one can see from most of the numerical results (see figures 4, 5 and 6) that significant class II activity initially appears to accompany high levels of class I disturbances. In contrast to their reasoning, our results indicate that whenever the initial level of class I disturbances is substantially higher than that of class II, class I wave components seem to suppress the three-dimensional (class II) components. These results contradict the hypothesis of the trigger mechanism. Figures 5 and 6 show that the conditions for the above suppression also include the initial phase angles of the various disturbances.

For extremely steep waves the water surface becomes three-dimensional even in the initial stage, see figure 1; this fact is in agreement with Su (1982) and Su *et al.* (1982). Their experimental observations show that in these cases the waves break soon afterwards.

Appendix

n	k_n	χ_n	$\tilde{B}_n$
Second order			
$n=5+5(j-1)+k$	k_j+k_k	$-\omega_j-\omega_k$	$-V^{(1)}_{n,j,k}\tilde{B}_j\tilde{B}_k/(\omega_n-\omega_j-\omega_k)$
$n=30+5(j-1)+k$	$-k_j+k_k$	$\omega_j-\omega_k$	$-V^{(2)}_{n,j,k}\tilde{B}^*_j\tilde{B}_k/(\omega_n+\omega_j-\omega_k)$
$n=55+5(j-1)+k$	$-k_j-k_k$	$\omega_j+\omega_k$	$-V^{(3)}_{n,j,k}\tilde{B}^*_j\tilde{B}^*_k/(\omega_n+\omega_j+\omega_k)$
Third order			
$n=80+25(j-1)+5(k-1)+l$	$k_j+k_k+k_l$	$-\omega_j-\omega_k-\omega_l$	$-\tilde{T}^{(1)}_{n,j,k,l}\tilde{B}_j\tilde{B}_k\tilde{B}_l/(\omega_n-\omega_j-\omega_k-\omega_l)$
$n=205+25(j-1)+5(k-1)+l$	$-k_j+k_k+k_l$	$\omega_j-\omega_k-\omega_l$	$-\tilde{T}^{(2)}_{n,j,k,l}\tilde{B}^*_j\tilde{B}_k\tilde{B}_l/(\omega_n+\omega_j-\omega_k-\omega_l)$
$n=330+25(j-1)+5(k-1)+l$	$-k_j-k_k+k_l$	$\omega_j+w_k-\omega_l$	$-\tilde{T}^{(3)}_{n,j,k,l}\tilde{B}^*_j\tilde{B}^*_k\tilde{B}_l/(\omega_n+\omega_j+\omega_k-\omega_l)$
$n=455+25(j-1)+5(k-1)+l$	$-k_j-k_k-k_l$	$\omega_j+\omega_k+\omega_l$	$-\tilde{T}^{(4)}_{n,j,k,l}\tilde{B}^*_j B^*_k\tilde{B}^*_l/(\omega_n+\omega_j+\omega_k+\omega_l)$
Fourth order			
$n=580+125(j-1)+25(k-1)+5(l-1)+m$	$k_j+k_k+k_l+k_m$	$-\omega_j-\omega_k-\omega_l-\omega_m$	$-\tilde{U}^{(1)}_{n,j,k,l,m}\tilde{B}_j\tilde{B}_k\tilde{B}_l\tilde{B}_m$ $/(\omega_n-\omega_j-\omega_k-\omega_l-\omega_m)$
$n=1205+125(j-1)+25(k-1)+5(l-1)+m$	$-k_j+k_k+k_l+k_m$	$\omega_j-\omega_k-\omega_l-\omega_m$	$-\tilde{U}^{(2)}_{n,j,k,l,m}\tilde{B}^*_j\tilde{B}_k\tilde{B}_l\tilde{B}_m$ $/(\omega_n+\omega_j-\omega_k-\omega_l-\omega_m)$
$n=1830+125(j-1)+25(k-1)+5(l-1)+m$	$-k_j-k_k+k_l+k_m$	$\omega_j+\omega_k-\omega_l-\omega_m$	$-\tilde{U}^{(3)}_{n,j,k,l,m}\tilde{B}^*_j\tilde{B}^*_k\tilde{B}_l\tilde{B}_m$ $/(\omega_n+\omega_j+\omega_k-\omega_l-\omega_m)$
$n=2455+125(j-1)+25(k-1)+5(l-1)+m$	$-k_j-k_k-k_l+k_m$	$\omega_j+\omega_k+\omega_l-\omega_m$	$-\tilde{U}^{(4)}_{n,j,k,l,m}\tilde{B}^*_j\tilde{B}^*_k\tilde{B}^*_l\tilde{B}_m$ $/(\omega_n+\omega_j+\omega_k+\omega_l-\omega_m)$
$n=3080+125(j-1)+25(k-1)+5(l-1)+m$	$-k_j-k_k-k_l-k_m$	$\omega_j+\omega_k+\omega_l+\omega_m$	$-\tilde{U}^{(5)}_{n,j,k,l,m}\tilde{B}^*_j\tilde{B}^*_k\tilde{B}^*_l\tilde{B}^*_m$ $/(\omega_n+\omega_j+\omega_k+\omega_l+\omega_m)$

TABLE 1. $n = 5, 6, \ldots, 3705; j, k, l, m = 1, 2, 3, 4, 5.$

Note that for a few cases where the expression in the denominator of $\tilde{B}_n$ in table 1 is of order $(k_0 a_0)^2$ and which correspond to near resonance conditions, $\tilde{B}_n$ was taken to be zero: this is in accordance with the definition of B'' and B''' given in Stiassnie & Shemer (1984). All the kernels are given in the above-mentioned paper except for $\tilde{U}^{(1)}$, $\tilde{U}^{(4)}$ and $\tilde{U}^{(5)}$. It turns out that the terms which include $\tilde{U}^{(1)}$ and $\tilde{U}^{(5)}$ do not contribute to the final results in the present paper. The expression for $\tilde{U}^{(4)}$ is:

$$
\begin{aligned}
\tilde{U}^{(4)}_{0,1,2,3,4} = X^{(4)}_{0,1,2,3,4} &+ \frac{V^{(1)}_{0,-1-2,4-3}V^{(2)}_{4-3,3,4}V^{(3)}_{-1-2,1,2}}{(\omega_{-1-2}+\omega_1+\omega_2)(\omega_{4-3}+\omega_3-\omega_4)} \\
&+ \frac{V^{(1)}_{0,4-1,-2-3}V^{(2)}_{4-1,1,4}V^{(3)}_{-2-3,2,3}}{(\omega_{4-1}+\omega_1-\omega_4)(\omega_{-2-3}+\omega_2+\omega_3)} + \frac{V^{(2)}_{0,1+2,4-3}V^{(1)}_{1+2,1,2}V^{(2)}_{4-3,3,4}}{(\omega_{1+2}-\omega_1-\omega_2)(\omega_{4-3}+\omega_3-\omega_4)} \\
&+ \frac{V^{(2)}_{0,1-4,-2-3}V^{(2)}_{4-1,1,4}V^{(3)}_{-2-3,2,3}}{(\omega_{1-4}+\omega_4-\omega_1)(\omega_{-2-3}+\omega_2+\omega_3)} + \frac{V^{(3)}_{0,1+2,3-4}V^{(1)}_{1+2,1,2}V^{(2)}_{3-4,4,3}}{(\omega_{1+2}-\omega_1-\omega_2)(\omega_{3-4}+\omega_4-\omega_3)} \\
&+ \frac{V^{(3)}_{0,1-4,2+3}V^{(2)}_{1-4,4,1}V^{(1)}_{2+3,2,3}}{(\omega_{1-4}+\omega_4-\omega_1)(\omega_{2+3}-\omega_2-\omega_3)} - \frac{V^{(1)}_{0,4,-1-2-3}T^{(4)}_{-1-2-3,1,2,3}}{\omega_{-1-2-3}+\omega_1+\omega_2+\omega_3} \\
&- \frac{V^{(1)}_{0,-1-2-3,4}T^{(4)}_{-1-2-3,1,2,3}}{\omega_{-1-2-3}+\omega_1+\omega_2+\omega_3} - \frac{V^{(2)}_{0,1,4-2-3}T^{(3)}_{4-2-3,2,3,4}}{\omega_{4-2-3}+\omega_2+\omega_3+\omega_4} \\
&- \frac{V^{(2)}_{0,1+2+3,4}T^{(1)}_{1+2+3,1,2,3}}{\omega_{1+2+3}-\omega_1-\omega_2-\omega_3} - \frac{V^{(3)}_{0,1,2+3-4}T^{(2)}_{2+3-4,4,2,3}}{\omega_{2+3-4}+\omega_4-\omega_2-\omega_3} \\
&- \frac{V^{(3)}_{0,2+3-4,1}T^{(2)}_{2+3-4,4,2,3}}{\omega_{2+3-4}+\omega_4-\omega_2-\omega_3} - \frac{W^{(2)}_{0,1,-2-3,4}V^{(3)}_{-2-3,2,3}}{\omega_{-2-3}+\omega_2+\omega_3} \\
&- \frac{W^{(2)}_{0,1,4,-2-3}V^{(3)}_{-2-3,2,3}}{\omega_{-2-3}+\omega_2+\omega_3} - \frac{W^{(3)}_{0,2+3,1,4}V^{(1)}_{2+3,2,3}}{\omega_{2+3}-\omega_2-\omega_3} \\
&- \frac{W^{(3)}_{0,1,2+3,4}V^{(1)}_{2+3,2,3}}{\omega_{2+3}-\omega_2-\omega_3} - \frac{W^{(3)}_{0,1,2,4-3}V^{(2)}_{4-3,3,4}}{\omega_{4-3}+\omega_3-\omega_4} - \frac{W^{(4)}_{0,3-4,1,2}V^{(2)}_{3-4,4,3}}{\omega_{3-4}+\omega_4+\omega_3} \\
&- \frac{W^{(4)}_{0,1,3-4,2}V^{(2)}_{3-4,4,3}}{\omega_{3-4}+\omega_4-\omega_3} - \frac{W^{(4)}_{0,1,2,3-4}V^{(2)}_{3-4,4,3}}{\omega_{3-4}+\omega_4-\omega_3}.
\end{aligned}
$$

REFERENCES

JAMES, M. L., SMITH, G. M. & WOLFORD, J. C. 1977 *Applied Numerical Methods for Digital Computation with FORTRAN and CSMP*. Harper & Row.

LAKE, B. M., YUEN, H. C., RUNGALDIER, H. & FERGUSON, W. E. 1977 Nonlinear deep water waves: theory and experiments. 2. Evolution of a continuous wave train. *J. Fluid Mech.* **83**, 49–74.

McLEAN, J. W. 1982 Instabilities of finite-amplitude water waves *J. Fluid Mech.* **114**, 315–330.

MILDER, D. M. 1977 A note regarding 'On Hamilton's principle for surface waves'. *J. Fluid Mech.* **83**, 159–161.

MILES, J. W. 1977 On Hamilton's principle for surface waves. *J. Fluid Mech.* **83**, 153–158.

SHEMER, L. & STIASSNIE, M. 1985 Initial instability and long-time evolution of Stokes waves. In *The Ocean Surface: Wave Breaking, Turbulent Mixing and Radio Probing* (ed. Y. Toba & H. Mitsuyasu), pp. 51–57. D. Reidel.

STIASSNIE, M. & KROSZYNSKI, U. I. 1982 Long-time evolution of an unstable water-wave train. *J. Fluid Mech.* **116**, 207–225.

STIASSNIE, M. & SHEMER, L. 1984 On modifications of the Zakharov equation for surface gravity waves. *J. Fluid Mech.* **143**, 47–67.

SU, M.-Y. 1982 Three-dimensional deep-water waves. Part I. Experimental measurement of skew and symmetric wave patterns. *J. Fluid Mech.* **124**, 73–108.

SU, M.-Y., BERGIN, M., MARLER, P. & MYRICK, R. 1982 Experiments on non-linear instabilities and evolution of steep gravity-wave trains. *J. Fluid Mech.* **124**, 45–72.

SU, M.-Y. & GREEN, A. W. 1984 Coupled two-and three-dimensional instabilities of surface gravity waves. *Phys. Fluids* **27**, 2595–2597.

SU, M.-Y. & GREEN, A. W. 1985 Wave breaking and nonlinear instability coupling. In *The Ocean Surface: Wave Breaking, Turbulent Mixing and Radio Probing* (ed. Y. Toba & H. Mitsuyasu). D. Reidel.

YUEN, H. C. & LAKE, B. M. 1982 Nonlinear dynamics of deep-water gravity waves. *Adv. Appl. Mech.* **22**, 67–229.

ZAKHAROV, V. E. 1968 Stability of periodic waves of finite amplitude on the surface of a deep fluid. *J. Appl. Mech. Tech. Phys.* (Engl. transl.) **9**, 190–194.

2.23